

# All-Solid-State Lithium Organic Battery with Composite Polymer Electrolyte and Pillar[5]quinone Cathode

Zhiqiang Zhu,<sup>†</sup> Meiling Hong,<sup>†</sup> Dongsheng Guo,<sup>†</sup> Jifu Shi,<sup>‡</sup> Zhanliang Tao,<sup>†</sup> and Jun Chen<sup>\*,†</sup>

<sup>†</sup>Key Laboratory of Advanced Energy Materials Chemistry (Ministry of Education) and State Key Laboratory of Elemento-Organic Chemistry, Collaborative Innovation Center of Chemical Science and Engineering, College of Chemistry, Nankai University, Tianjin 300071, China

<sup>‡</sup>Key Laboratory of Renewable Energy & Gas Hydrate, Guangzhou Institute of Energy Conversion, Chinese Academy of Sciences, Guangzhou 510640, China

## S Supporting Information

**ABSTRACT:** The cathode capacity of common lithium ion batteries (LIBs) using inorganic electrodes and liquid electrolytes must be further improved. Alternatively, all-solid-state lithium batteries comprising the electrode of organic compounds can offer much higher capacity. Herein, we successfully fabricated an all-solid-state lithium battery based on organic pillar[5]quinone (C<sub>35</sub>H<sub>20</sub>O<sub>10</sub>) cathode and composite polymer electrolyte (CPE). The poly(methacrylate) (PMA)/poly(ethylene glycol) (PEG)-LiClO<sub>4</sub>-3 wt % SiO<sub>2</sub> CPE has an optimum ionic conductivity of 0.26 mS cm<sup>-1</sup> at room temperature. Furthermore, pillar[5]quinone cathode in all-solid-state battery rendered an average operation voltage of ~2.6 V and a high initial capacity of 418 mAh g<sup>-1</sup> with a stable cyclability (94.7% capacity retention after 50 cycles at 0.2C rate) through the reversible redox reactions of enolate/quinonid carbonyl groups, showing favorable prospect for the device application with high capacity.

Lithium ion batteries (LIBs) with liquid electrolytes have gained huge success in portable electronics in the last three decades.<sup>1–3</sup> However, current LIBs have a bottleneck in capacity of electrode active materials mainly due to the low practical capacities of commonly used inorganic lithium-transition-metal-oxide cathodes (<170 mAh g<sup>-1</sup>) and graphite anode (~370 mAh g<sup>-1</sup>).<sup>4–7</sup> Thus, new electrodes with high specific capacity need to be developed. On the anode site, solid-state lithium battery using high capacity lithium (~3800 mAh g<sup>-1</sup>) has the potential to improve the energy density.<sup>8</sup> On the cathode side, organic carbonyl compounds have recently attracted much attention owing to their high theoretical gravimetric capacities and resource renewability.<sup>9–11</sup> Unfortunately, organic materials with low molecular weight usually exhibit poor cyclability because of their high solubility in aprotic electrolyte.<sup>12–14</sup> To overcome this issue, attempts including anchoring, polymerization, or salt formation of the active materials have been proposed, and achievements have been obtained.<sup>15–19</sup> Meanwhile, the appealing thing is that several recent reports have proved that replacing traditional liquid electrolyte with quasi-solid-state electrolyte is also effective,<sup>20–23</sup> which enables the fabrication of solid-state batteries with lithium anode and organic cathode with high capacity.

However, so far, only few studies in this field have been done, and the investigated electrolyte and cathode are very limited. For example, quasi-solid batteries based on a silica room-temperature ionic liquid (RTIL) composite polymer electrolyte (CPE) and several organic cathode compounds have been proposed to render prolonged life-span (10–200 cycles) with stable capacities in the range of 200–300 mAh g<sup>-1</sup>.<sup>20–22</sup> Our group recently developed a poly(methacrylate) (PMA)/poly(ethylene glycol) (PEG)-based gel polymer electrolyte (GPE) for quasi-solid lithium batteries.<sup>23</sup> When using calix[4]quinone as the cathode, the quasi-solid-state battery delivered a capacity of 379 mAhg<sup>-1</sup> after 100 cycles. In spite of this promising result, the presence of conventional liquid electrolyte components in this GPE is believed to be harmful for battery performance.<sup>24,25</sup> Thus, developing more reliable all-solid-state electrolyte as well as high capacity cathode to produce all-solid-state lithium organic batteries is of significant importance.

Despite the advantage that organic carbonyl compounds can possess high theoretical gravimetric capacities by combining large carbonyl number and low molecular weight,<sup>14</sup> the densely incorporated carbonyl groups usually lead to low active site unitization as well as practical capacity.<sup>26,27</sup> In contrast, macrocyclic molecules such as calixquinone equipped with several *p*-quinone units could realize high efficiency for the use of the active sites because of their unique macrocyclic structure.<sup>15,23</sup> We note that a new macrocycle, pillar[5]quinone (P5Q), containing five quinone units linked by methylene bridges at para positions,<sup>28–30</sup> can offer a high theoretical capacity of 446 mAh g<sup>-1</sup>. Furthermore, the pillar architecture of P5Q should be favorable to Li uptake. Therefore, in this study we selected P5Q as the cathode of all solid-state lithium organic batteries.

The research on polymer electrolytes began since the discovery of ionic conductivity in a PEO/Na<sup>+</sup> complex in 1973.<sup>31</sup> However, dry solid polymer electrolyte (DSPE) systems comprising of a complex of polymer matrix and lithium salts generally exhibit very low ionic conductivity at room temperature (in the order of 10<sup>-6</sup> S cm<sup>-1</sup>). There are two ways to improve the ionic conductivity. One is introducing liquid plasticizers into DSPE systems to generate GPE.<sup>32</sup> The other is adding ceramic fillers into the polymer electrolyte to

Received: July 31, 2014

Published: November 10, 2014



form CPE.<sup>33–35</sup> Recently, we developed a PMA/PEG-based GPE for quasi-solid-state battery application based on the former concept.<sup>23</sup> However, a large amount of liquid electrolytes is needed in this system, which might be evaporated at high temperature and thus would lower the conductivity.<sup>24</sup> Considering the high mobility and good solvating ability of the polymer hybrid, we are encouraged to further investigate its application in the more reliable CPE system to avoid this issue.

Here we report an all-solid-state lithium organic battery that features both high specific capacity and good stability. A new CPE based on PMA/PEG-LiClO<sub>4</sub>-SiO<sub>2</sub> has been prepared, exhibiting a maximum ionic conductivity of 0.26 mS cm<sup>-1</sup> with 3 wt % SiO<sub>2</sub> at room temperature. Furthermore, by coupling the optimized CPE with a high capacity PSQ cathode, a solid cell has been successfully fabricated. In this system, the cathode offered an initial capacity of 418 mAh g<sup>-1</sup> with an average operating voltage of ~2.6 V and 94.7% capacity retention after 50 cycles at 0.2C rate.

Our previous work has confirmed the applicability of PMA/PEG-based polymer matrices for utilization in quasi-solid-state GEP.<sup>23</sup> Herein, to obtain satisfied ionic conductivity without incorporating liquid plasticizer, nanosized TiO<sub>2</sub> and SiO<sub>2</sub> (Figure S1) have been introduced in the polymer matrices. Four types of CPE, including PMA-LiClO<sub>4</sub>-TiO<sub>2</sub>, PMA-LiClO<sub>4</sub>-SiO<sub>2</sub>, PMA/PEG-LiClO<sub>4</sub>-TiO<sub>2</sub>, PMA/PEG-LiClO<sub>4</sub>-SiO<sub>2</sub>, were prepared in this work. The detailed fabrication process is described in the Supporting Information (SI). To improve the particle dispersion as well as the stability of CPE, sonication is employed to enhance the interaction between the particles and the polymer.

We first investigated the effects of the filler contents on the ion conductivity of these electrolytes at room temperature. As shown in Figure 1a, all electrolytes show similar conductivity trends, i.e., the conductivity increases first and reduces afterward with the increase of the filler contents. The nonlinear effect of particle content on conductivity is analogous to the result observed in previous reports.<sup>36–38</sup> On one hand, the introduction of nanoparticles could not only enhance the polymer amorphicity but also add free volume and stimulate segmental dynamics.<sup>33,39</sup> On the other hand, the added oxide could promote the dissociation of lithium salts by the interaction between LiClO<sub>4</sub> and the surface of the nanoparticles and result in higher free ion concentration.<sup>35,40</sup> Thus, the formation of percolative particle network should contribute the improved conductivity in the low filler content. However, further increase of filler concentration will block the percolation and cause volume depletion, thus lowering the ionic conductivity.<sup>35,40</sup> Therefore, a maximum conductivity will be achieved at intermediate filler content. Here, the optimal content is 3 wt % for all electrolytes, which should be originated from the utilization of high aspect ratio particles that enables percolation of particles at low loading.<sup>35</sup>

Besides, irrespective of the filler content, the ionic conductivity is constantly better with SiO<sub>2</sub> than TiO<sub>2</sub> filler. This should be attributed to the following three reasons: First, the smaller size of SiO<sub>2</sub> (7–10 nm) compared to TiO<sub>2</sub> (20–30 nm) is more favorable to reduce the polymer crystallinity and thus enhance the segmental motion.<sup>39</sup> Second, as the particle surface could also provide an additional ion transport pathway, the high aspect ratio should give SiO<sub>2</sub> advantage in ion migration.<sup>35</sup> Third, the acid SiO<sub>2</sub> helps ion-pair dissociation and thus results in an enhanced Li<sup>+</sup> concentration as well as ionic conductivity.<sup>36</sup> Meanwhile, it should be pointed out that the

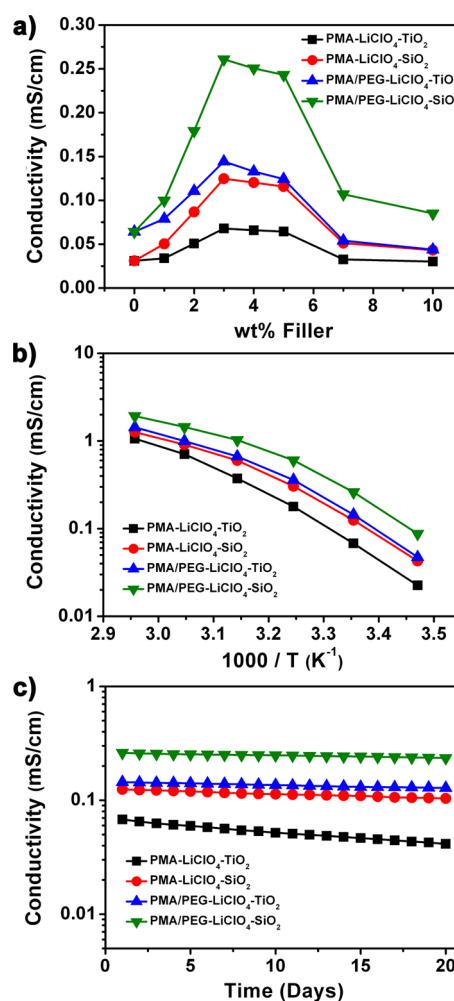


**Figure 1.** (a) Influence of fillers contents on the ionic conductivity of the electrolytes at room temperature. (b) Temperature dependence of the ionic conductivity of the electrolytes with 3 wt % fillers. (c) Changes upon time of the conductivity of the electrolytes with 3 wt % fillers at room temperature. Data obtained by impedance spectroscopy measurements.

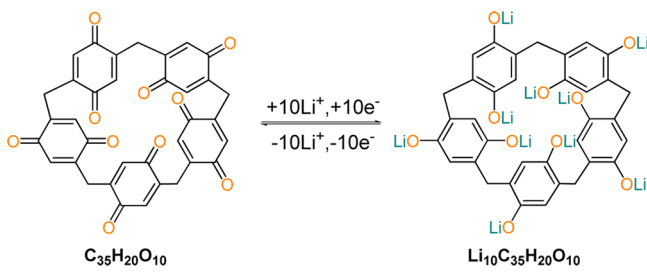
highly mobile polymer chain segments in PEG could also facilitate the ionic transportation.<sup>25,34</sup> A maximum conductivity of 0.26 mS cm<sup>-1</sup> was obtained by PMA/PEG-LiClO<sub>4</sub>-3 wt % SiO<sub>2</sub>. This value meets the basic requirement of LIBs<sup>24</sup> and is even comparable to the reported value of GPEs.<sup>23</sup>

Figure 1b shows the temperature dependence of the ionic conductivity of the four types of CPE with the optimized filler content (3 wt %). Notably, the conductivity decreases slowly even in the low temperature range. The relative high conductivity is due to the addition of nanoparticles which could significantly prevent the well-known crystalline–amorphous transition of the polymer matrix.<sup>33</sup> As a result, the PMA/PEG-LiClO<sub>4</sub>-SiO<sub>2</sub> system can provide consistently high conductivity in a wide temperature range of 15–65 °C, which is benefit for practical application. The time evolution of the room-temperature conductivity of these CPEs is presented in Figure 1c, demonstrating good stability. Considering the fact that PMA/PEG-LiClO<sub>4</sub>-3 wt % SiO<sub>2</sub> exhibited the highest conductivity, it was chosen for further electrochemical investigation.

In pursuit of high energy density, an organic cathode of PSQ with high theoretical capacity has been selected. The macro-

cyclic structure of P5Q is expected to favor Li uptake. The target P5Q ( $C_{35}H_{20}O_{10}$ , Scheme 1) was synthesized from the

### Scheme 1. Structure and Proposed Electrochemical Redox Mechanism of P5Q



purchased material *p*-dimethoxybenzene (Sigma-Aldrich) in two steps according to previous reports:<sup>28,41</sup> cyclization and oxidation (detailed in SI). NMR and MS spectra were used to characterize the structure of obtained sample, confirming the formation of P5Q. The product was in the form of pale yellow powders and showed columnar morphology in the micron dimension (Figure S2). To enhance its electronic conductivity, some activated graphene has been added during the fabrication of the electrode.

The electrode performance of P5Q was first evaluated in traditional liquid electrolytes (1 M  $LiPF_6$  in ethylene carbonate:diethyl carbonate solutions (1:1 in volume)). The cathode composition and cell assembly procedures are detailed in SI. The characterization of the cathode and CPE films is shown in Figure S3. As expected, P5Q can provide a high initial capacity of  $\sim 409$   $mAh\ g^{-1}$ , corresponding to 91.7% of its theoretical capacity ( $446$   $mAh\ g^{-1}$ ) (Figure S4). Such a high capacity is an indicative of high utilization of active carbonyl benefited from its unique pillar architecture. Nevertheless, the cycling test revealed rapid capacity fading, which should be ascribed to the seriously dissolution of active materials into the liquid electrolyte. To avoid such problem, the liquid electrolyte was replaced with the prepared PMA/PEG- $LiClO_4$ -3 wt %  $SiO_2$  CPE.

Figure 2 shows the electrochemical performance of the all-solid-state battery with PMA/PEG- $LiClO_4$ -3 wt %  $SiO_2$  CPE and P5Q cathode. The charge–discharge profiles are similar to that obtained in liquid electrolyte (Figure 2a), manifesting that the prepared solid-state electrolyte does not change the redox activity of P5Q. During the discharge process, the slope plateau from  $\sim 2.9$  to 2.5 V should be related to the multistep reduction of the carbonyl groups in the quinone units, while the slope plateau in the charge profile corresponds to the reoxidation of the enolate groups (Scheme 1).<sup>23</sup> More excitingly, the cell can still render an initial capacity of  $418$   $mAh\ g^{-1}$ . Furthermore, unlike in the liquid cell case, the solid cell demonstrates satisfactory cyclability. After 50 cycles at 0.2C rate ( $89.2$   $mA\ g^{-1}$ ), 94.7% of the initial capacity ( $396$   $mAh\ g^{-1}$ ) can be retained (Figure 2b), which is superior to that obtained in quasi-solid-state battery.<sup>23</sup> This improved cyclability stems from the better interfacial stability of CPE compared to that of GPE.<sup>42</sup> The Coulombic efficiency is close to 99% during the whole cycling test. The rate capability of this solid cell is also passable (Figure 2c). The capacities obtained at 0.3, 0.5, and 1C are 361, 286, and 197  $mAh\ g^{-1}$ , respectively. These results indicate that the proposed solid electrolyte has good compatibility to the organic electrode.

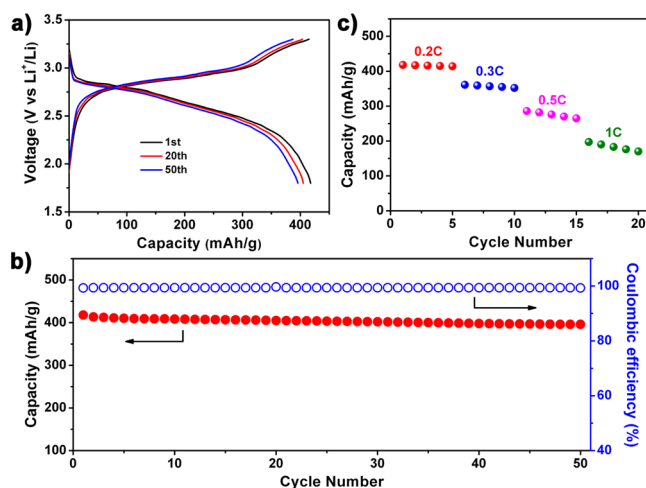


**Figure 2.** Electrochemical performance of the all-solid-state cell with P5Q cathode and PMA/PEG- $SiO_2$  GPE: (a) typical discharge–charge profiles at 0.2C rate; (b) the cycling performance between 1.8 and 3.3 V at 0.2C rate; and (c) rate capability.

Based on the obtained high capacity and improved cyclability, the all-solid-state lithium battery provides a general strategy for high capacity organic materials toward high energy batteries. Given that the initial capacity of  $418$   $mAh\ g^{-1}$ , the energy density of the P5Q electrode is as high as  $1086$   $Wh\ kg^{-1}$  only considering the active material. This is nearly twice that of common intercalation compounds such as  $LiFePO_4$  and  $LiMn_2O_4$  ( $\sim 580$  and  $590$   $Wh\ kg^{-1}$ , respectively). Even counting their fractions in the electrodes ( $\sim 55$  wt % for P5Q and  $\sim 90$  wt % for  $LiFePO_4$  and  $LiMn_2O_4$ ), the energy density of P5Q cathode is still  $\sim 10\%$  higher ( $\sim 600$   $Wh\ kg^{-1}$ ). Note that this value can be further improved by optimizing the electrode composition. As an attempt, a cathode containing 70 wt % P5Q has been tested, and an initial capacity of  $\sim 405$   $mAh\ g^{-1}$  was obtained (Figure S5). Therefore, the energy density per cathode composite reaches  $\sim 740$   $Wh\ kg^{-1}$ . Considering the specific capacity ( $3860$   $mAh\ g^{-1}$ ) of lithium anode<sup>25</sup> and assuming a one-third reduction factor associated with the weight of battery ancillary components,<sup>43</sup> an energy density of  $\sim 230$   $Wh\ kg^{-1}$  is expected for the battery, which is about 90% higher than that calculated for common inorganic lithium-transition-metal-oxide cathodes/graphite systems (Table S1, see calculated details in the SI). These features, along with the abundance of organic materials, make this type of all-solid-state lithium organic battery very promising for lithium batteries, even though the volumetric energy density of the P5Q cathode as well as the battery would be relative low due to its low density (Table S2).

In conclusion, a new PMA/PEG-based nanocomposite polymer electrolyte has been prepared in this work. After optimization, the PMA/PEG-based CPE with 3 wt %  $SiO_2$  (7–10 nm) exhibited an ionic conductivity of  $0.26$   $mS\ cm^{-1}$  at room temperature. By selecting a high capacity carbonyl compound cathode, P5Q, an all-solid-state lithium organic battery has been successfully fabricated. The cathode with 55 wt % P5Q rendered an average operation voltage of 2.6 V and an initial capacity as high as  $418$   $mAh\ g^{-1}$  at 0.2C rate with 94.7% capacity retention after 50 cycles. Our results reveal the promising future of all-solid-state lithium organic battery.

**■ ASSOCIATED CONTENT****■ Supporting Information**

Synthesis of the solid polymer electrolytes. Experimental procedures and characterization data of P5Q. Electrochemical measurements of the assembled battery. This material is available free of charge via the Internet at <http://pubs.acs.org>.

**■ AUTHOR INFORMATION****Corresponding Author**

chenabc@nankai.edu.cn

**Notes**

The authors declare no competing financial interest.

**■ ACKNOWLEDGMENTS**

This study was supported by the National Programs of 973 (2011CB935900), NSFC (21231005, 51231003), and MOE (B12015, IRT13R30, and 113016A).

**■ REFERENCES**

- (1) Armand, M.; Tarascon, J. M. *Nature* **2008**, *451*, 652–657.
- (2) Chen, J.; Cheng, F. *Acc. Chem. Res.* **2009**, *42*, 713–723.
- (3) Goodenough, J. B.; Park, K. S. *J. Am. Chem. Soc.* **2013**, *135*, 1167–1176.
- (4) Scrosati, B.; Garche, J. *J. Power Sources* **2010**, *195*, 2419–2430.
- (5) Ellis, B. L.; Lee, K. T.; Nazar, L. F. *Chem. Mater.* **2010**, *22*, 691–714.
- (6) Hernandez-Burgos, K.; Rodriguez-Calero, G. G.; Zhou, W.; Burkhardt, S. E.; Abruna, H. D. *J. Am. Chem. Soc.* **2013**, *135*, 14532–14535.
- (7) Etacheri, V.; Marom, R.; Elazari, R.; Salitra, G.; Aurbach, D. *Energy Environ. Sci.* **2011**, *4*, 3243–3262.
- (8) Khurana, R.; Schaefer, J. L.; Archer, L. A.; Coates, G. W. *J. Am. Chem. Soc.* **2014**, *136*, 7395–7402.
- (9) Liang, Y.; Tao, Z.; Chen, J. *Adv. Energy Mater.* **2012**, *2*, 742–769.
- (10) Song, Z.; Zhou, H. *Energy Environ. Sci.* **2013**, *6*, 2280–2301.
- (11) Liang, Y.; Zhang, P.; Yang, S.; Tao, Z.; Chen, J. *Adv. Energy Mater.* **2013**, *3*, 600–605.
- (12) Chen, H.; Armand, M.; Demailly, G.; Dolhem, F.; Poizot, P.; Tarascon, J. M. *ChemSusChem* **2008**, *1*, 348–355.
- (13) Liu, K.; Zheng, J.; Zhong, G.; Yang, Y. *J. Mater. Chem.* **2011**, *21*, 4125–4131.
- (14) Liang, Y. L.; Zhang, P.; Chen, J. *Chem. Sci.* **2013**, *4*, 1330–1337.
- (15) Genorio, B.; Pirnat, K.; Cerc-Korosec, R.; Dominko, R.; Gaberscek, M. *Angew. Chem., Int. Ed.* **2010**, *49*, 7222–7224.
- (16) Han, X.; Chang, C.; Yuan, L.; Sun, T.; Sun, J. *Adv. Mater.* **2007**, *19*, 1616–1621.
- (17) Song, Z.; Zhan, H.; Zhou, Y. *Angew. Chem., Int. Ed.* **2010**, *49*, 8444–8448.
- (18) Nokami, T.; Matsuo, T.; Inatomi, Y.; Hojo, N.; Tsukagoshi, T.; Yoshizawa, H.; Shimizu, A.; Kuramoto, H.; Komae, K.; Tsuyama, H.; Yoshida, J. *J. Am. Chem. Soc.* **2012**, *134*, 19694–19700.
- (19) Wang, S.; Wang, L.; Zhang, K.; Zhu, Z.; Tao, Z.; Chen, J. *Nano Lett.* **2013**, *13*, 4404–4409.
- (20) Hanyu, Y.; Honma, I. *Sci. Rep.* **2012**, *2*, 453.
- (21) Hanyu, Y.; Ganbe, Y.; Honma, I. *J. Power Sources* **2013**, *221*, 186–190.
- (22) Hanyu, Y.; Sugimoto, T.; Ganbe, Y.; Masuda, A.; Honma, I. *J. Electrochem. Soc.* **2014**, *161*, A6–A9.
- (23) Huang, W.; Zhu, Z.; Wang, L.; Wang, S.; Li, H.; Tao, Z.; Shi, J.; Guan, L.; Chen, J. *Angew. Chem., Int. Ed.* **2013**, *52*, 9162–9166.
- (24) Quartarone, E.; Mustarelli, P. *Chem. Soc. Rev.* **2011**, *40*, 2525–2540.
- (25) Xu, W.; Wang, J.; Ding, F.; Chen, X.; Nasybulin, E.; Zhang, Y.; Zhang, J. *Energy Environ. Sci.* **2014**, *7*, 513–537.
- (26) Renault, S.; Geng, J.; Dolhem, F.; Poizot, P. *Chem. Commun.* **2011**, *47*, 2414–2416.
- (27) Geng, J.; Bonnet, J.-P.; Renault, S.; Dolhem, F.; Poizot, P. *Energy Environ. Sci.* **2010**, *3*, 1929–1933.
- (28) Cao, D.; Kou, Y.; Liang, J.; Chen, Z.; Wang, L.; Meier, H. *Angew. Chem., Int. Ed.* **2009**, *48*, 9721–9723.
- (29) Lao, K.; Yu, C. *J. Comput. Chem.* **2011**, *32*, 2716–2726.
- (30) Zhu, Z.; Guo, D.; Tao, Z.; Chen, J. *Sci. China: Chem.* **2014**, *44*, 1175–1180.
- (31) Fenton, D. E.; Parker, J. M.; Wright, P. V. *Polymer* **1973**, *14*, 589.
- (32) Song, J.; Wang, Y.; Wan, C. *J. Power Sources* **1999**, *77*, 183–197.
- (33) Scrosati, B.; Croce, F.; Appetecchi, G. B.; Persi, L. *Nature* **1998**, *394*, 456–458.
- (34) Quartarone, E. *Solid State Ionics* **1998**, *110*, 1–14.
- (35) Srivastava, S.; Schaefer, J. L.; Yang, Z.; Tu, Z.; Archer, L. A. *Adv. Mater.* **2014**, *26*, 201–234.
- (36) Bhattacharyya, A. J.; Maier, J. *Adv. Mater.* **2004**, *16*, 811–814.
- (37) Schaefer, J. L.; Yanga, D. A.; Archer, L. A. *Chem. Mater.* **2013**, *25*, 834–839.
- (38) Lu, Y.; Korf, K.; Kambe, Y.; Tu, Z.; Archer, L. A. *Angew. Chem., Int. Ed.* **2014**, *53*, 488–492.
- (39) Capuano, F.; Scrosati, B. *J. Electrochem. Soc.* **1991**, *138*, 1918–1922.
- (40) Bhattacharyya, A. J. *J. Phys. Chem. Lett.* **2012**, *3*, 744–750.
- (41) Ogoshi, T.; Kanai, S.; Fujinami, S.; Yamagishi, T.-a.; Nakamoto, Y. *J. Am. Chem. Soc.* **2008**, *130*, 5022–5023.
- (42) Kumar, B.; Scanlon, L. G. *J. Power Sources* **1994**, *52*, 261–268.
- (43) Hassoun, J.; Lee, K. S.; Sun, Y. K.; Scrosati, B. *J. Am. Chem. Soc.* **2011**, *133*, 3139–3143.